Proc. Nat. Acad. Sci. USA
Vol. 68, No. 4, pp. 841-845, April 1971

High-Resolution X-Ray Diffraction Patterns of Crystalline Transfer RNA That Show Helical Regions

SUNG HOU KIM, GARY QUIGLEY, F. L. SUDDATH, AND ALEXANDER RICH

Department of Biology, Massachusetts Institute of Technology, Cambridge, Mass. 02139

Communicated February 1, 1971

ABSTRACT **Yeast phenylalanyl transfer RNA crystallizes in a simple orthorhombic unit cell (a = 33.2, b = 56.1, c = 161 Å), and the crystal yields an x-ray diffraction pattern with a resolution of 2.3 Å. From an analysis of the packing in the unit cell it is concluded that the molecular dimensions are approximately 80 by 33 by 28 Å. The diffraction pattern viewed along the a-axis has a distribution characteristic of double-helical nucleic acids. However, this distribution is not found when the pattern is viewed along the b-axis. This has been interpreted as indicating that the double-helical portions of the transfer RNA molecule are approximately half a helical turn in length, and therefore can contain 4-7 base pairs. These results are consistent with the cloverleaf formulation of transfer RNA secondary structure.**

Transfer RNA (tRNA) occupies a central role in molecular biology since it is active at the interface between polynucleotide sequences in messenger RNA and amino acid sequences in proteins. In addition, the molecule may have important regulatory activities in phenomena as varied as viral infection, embryological development, and tumor formation. There is thus considerable interest in relating its molecular structure to biological function. The nucleotide sequence of many tRNA molecules have been determined and they are all compatible with the "cloverleaf" (1) secondary structure, in which the molecule has several short, double-helical, hydrogen-bonded stems containing 4–7 base pairs. Somewhat over 2 years ago it was found that tRNA molecules could be crystallized (2–5). This opened the possibility that the same type of x-ray diffraction analysis could be carried out on these molecules as has been successful with the crystalline proteins. One of the major difficulties encountered was that the tRNA crystals produced only low-resolution diffraction data. In this laboratory, our earliest crystals gave a resolution of approximately 20 Å (2). Subsequent improvements in crystallization methods led to a resolution of 6–7 Å (6). A study of the three-dimensional Patterson function, using the 12-Å data on crystals of *Escherichia coli* formylmethionyl-tRNA, yielded approximate molecular dimensions of 80 by 25 by 35 Å (6).

We have continued to search for a more suitable crystal form for diffraction analysis, with the aim of obtaining higher resolution data. Here we report that yeast phenylalanyl-tRNA crystallizes in a simple orthorhombic unit cell and the diffraction data has 2.3-Å resolution. The symmetry and the dimensions of this unit cell strikingly reinforce our earlier interpretation of the overall size and shape of the molecule. In addition, the diffraction pattern provides evidence for the existence of double-helical domains in the molecule that are oriented parallel to its long axis but that have a length of approximately one-half of a double-helical turn. This interpretation is consistent with the cloverleaf model.

METHODS

The crystals were prepared from yeast phenylalanyl-tRNA (Boehringer Manheim Corp.). In a typical crystallization protocol, 5–10 mg of tRNA was dissolved in 10 ml of 2 mM $MgCl_2$, and dialyzed extensively against a 2 mM $MgCl_2$ solution at 4°C. The tRNA was then precipitated with cold 95% ethanol, washed with acetone, and dried in a desiccator. The tRNA was redissolved to a concentration of 3–5 mg/ml in a buffered solution of 10 mM sodium cacodylate (pH 6.0)–10 mM $MgCl_2$–1 mM spermine hydrochloride. A 40-μl aliquot of the resultant solution was placed in each depression of a glass spot plate, and the plate was then sealed in a flat transparent plastic box that contained a precipitating solution. Crystallization occurred upon vapor-phase equilibration. The precipitating solutions were either 10% 2-propanol or 10–12% 2-methyl-2,4-pentanediol. The boxes were stored at 4–6°C, and the progress of crystallization was followed by microscopic observation without opening the containers.

In some cases crystals are observed after 12 hr; however, most frequently, crystals do not appear for several days or in some cases for as long as 2 weeks. Raising the alcohol concentration slightly tends to hasten crystal formation but yields smaller crystals. The crystals are usually small but occasion-

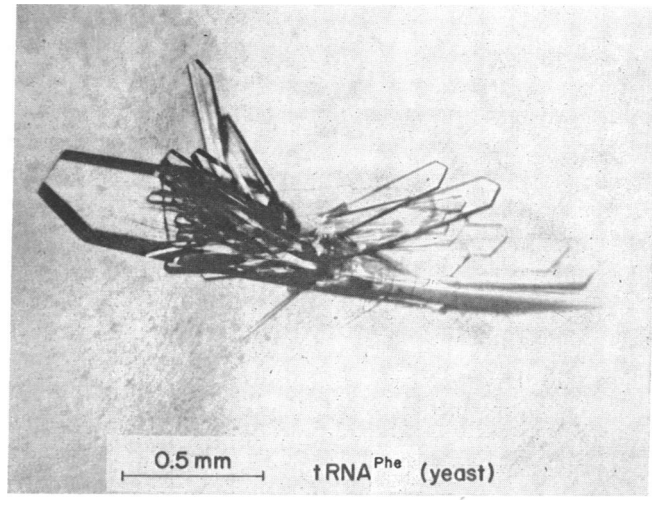

Fig. 1. A typical cluster of plate-like crystals of yeast tRNA^{Phe}. The crystals rarely appear isolated in these preparations.

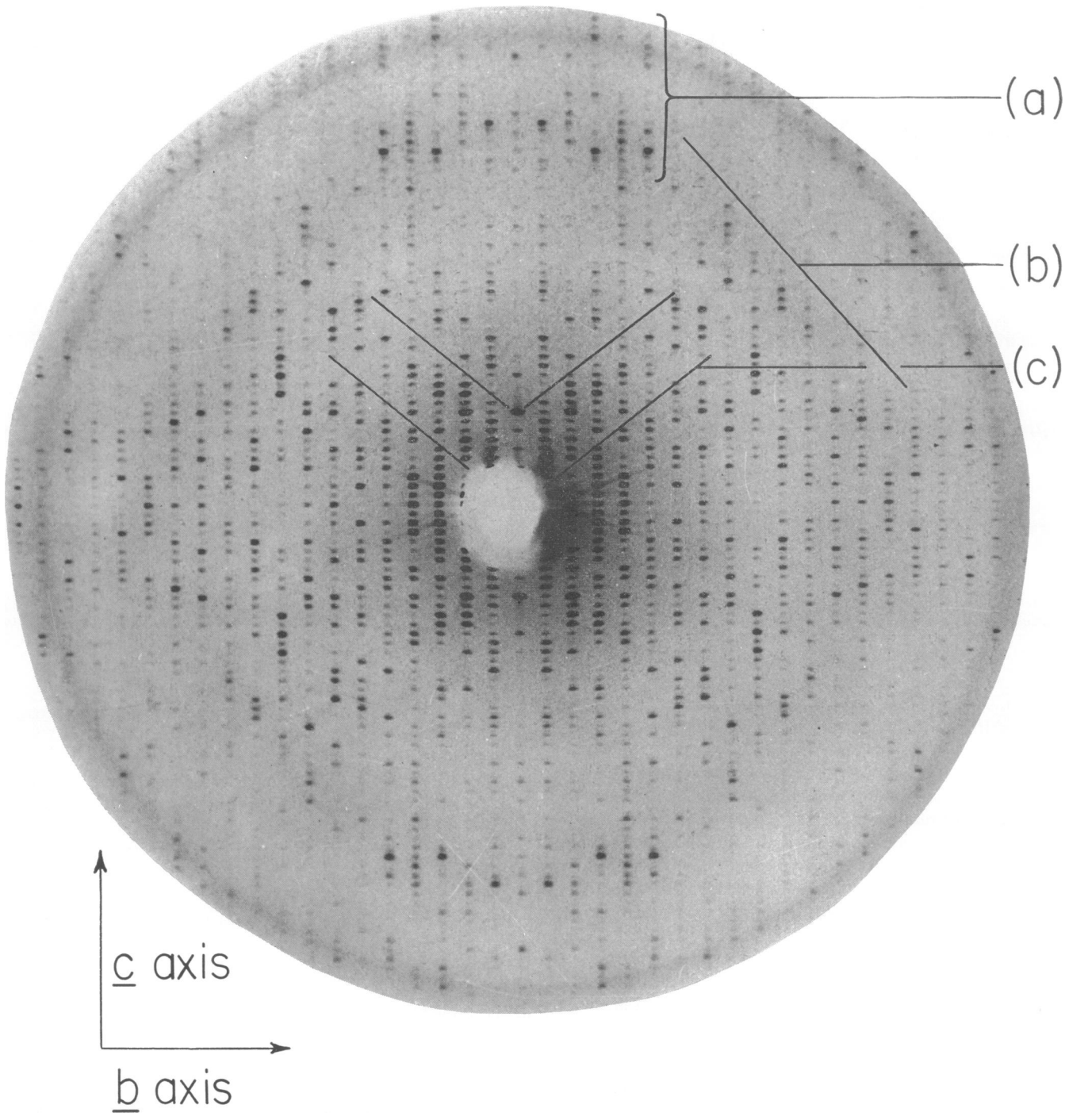

FIG. 2. Precession diffraction photograph of tRNA crystal along the *a*-axis. The crystal is the largest one visible in Fig. 1. It was mounted in a thin-walled quartz capillary with a droplet of mother liquid and was then sealed with wax. The exposure was 18 hr, and the precession angle was 15°. The region (*a*) represents 3- to 4-Å reflections on the meridian. Just below this is a region with few reflections. Lines of reflections (*b*) radiate downward and outward from this, producing a "diamond" effect for the overall pattern. A weaker exposure makes the cross-like distribution (*c*) around the origin more pronounced.

ally attain dimensions of 1–2 by 0.5 by 0.15 mm. They initially appear as fine needles or, more frequently, as thin plates which gradually thicken with time. A photomicrograph of these crystals is shown in Fig. 1.

RESULTS

X-ray diffraction patterns were taken on precession cameras using an Elliott rotating anode tube as an x-ray source. The crystals have an orthorhombic unit cell with dimensions a = 33.2 Å, b = 56.1 Å, and c = 161 Å. The space group is $P2_122_1$ with 1 molecule per asymmetric unit. The tRNA thus crystallizes in an elongated unit cell that is one molecule thick along the 33-Å axis. Because of the 2-fold axis perpendicular to the c axis, the length of the molecule is limited to 80 Å, with a head-to-head, tail-to-tail packing along the c direction. The unit cell has two molecules along the 56-Å axis. The overall

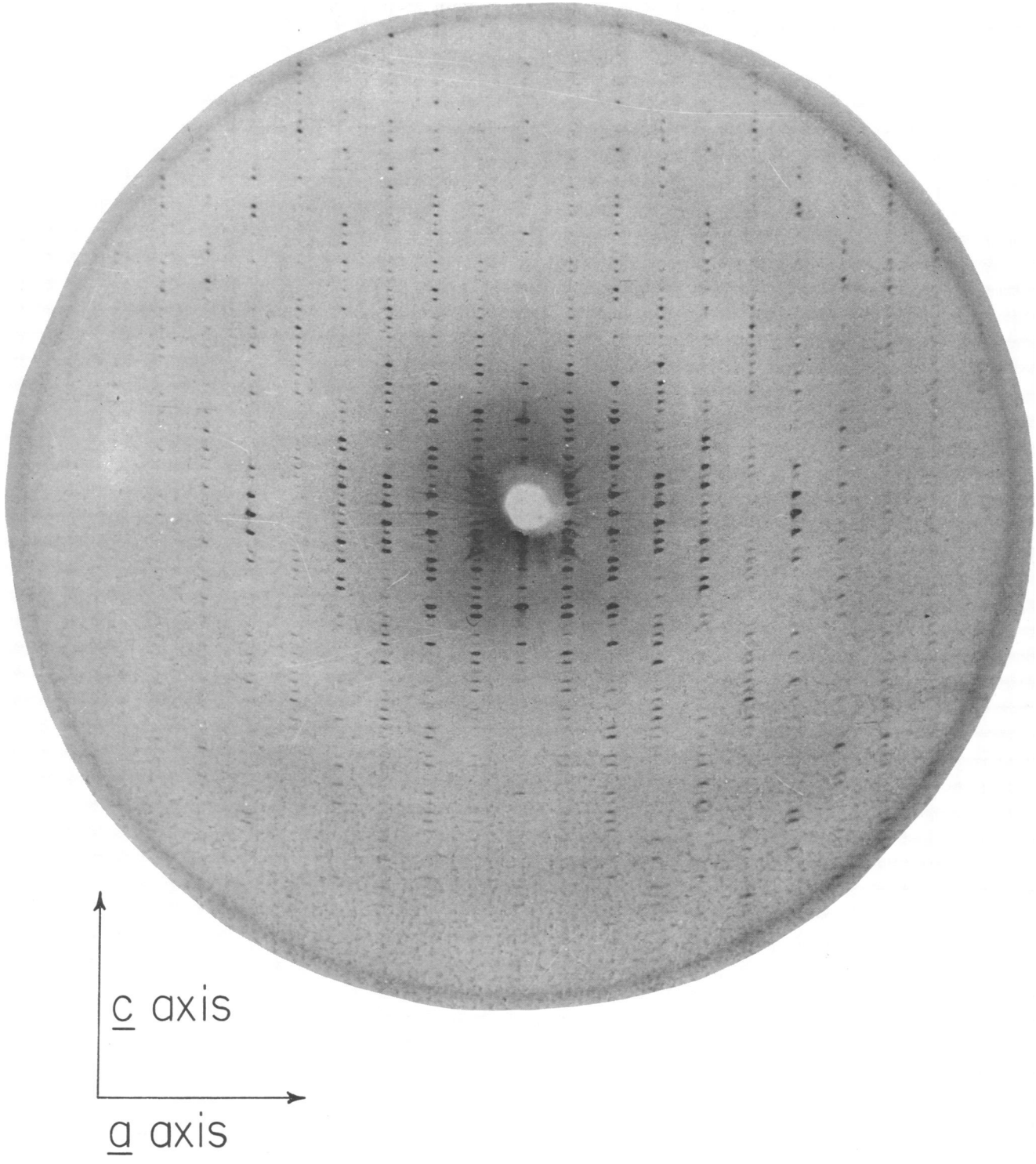

FIG. 3. Precession diffraction photograph of tRNA crystal along the *b*-axis. The exposure time was 17 hr and the precession angle 15°.

dimensions of the molecule thus agree rather closely with those deduced from the three-dimensional Patterson function calculated from the diffraction data of *E. coli* formyl-methionyl-tRNA crystals (6). However, the present measurements are more direct because of the symmetry constraints of the unit cell.

A diffraction pattern of these crystals is shown in Fig. 2. In this precession photograph, the x-ray beam is traveling along the 33-Å axis. The photograph has diffraction spots that extend out to 3.0 Å and are fully represented at this resolution. By changing the precession angle of the camera, we could show that the diffraction data extend out to a limit of 2.3 Å.

A diffraction photograph of a macromolecular crystal does not generally reveal much about the structure of the individual molecule since it represents diffraction data from the entire unit cell seen in projection. However, in this case the

unusual distribution of diffraction intensity allows us to draw some conclusions concerning the structure of the molecule. The pattern in Fig. 2 has a distribution of diffraction intensity that is characteristic of a helix (7). Diffraction from helical structures produces a cross-like distribution of diffraction intensity at the origin of the pattern, and a region on the meridian that has very little intensity. However, further out along the meridian there are usually intense reflections, with regions of intensity radiating downward and outwards from them toward the equator. In the case of helical nucleic acids, the near meridional reflections occur in the 3 to 4-Å region and arise from the stacked purine·pyrimidine base pairs (8). Reflections are seen in this area in Fig. 2(*a*). Radiating downwards are a row of reflections (*b*) that extend toward the equator of the pattern. Finally, the cross-like distribution of intensity is seen around the origin in the region labeled (*c*). Here we are drawing attention to features in the continuous Fourier transform of the unit cell as a whole as viewed along the *a*-axis. This pattern has many similarities to diffraction patterns obtained from fibrous polynucleotides of both natural and synthetic origin (8). In the fibrous nucleic acids, the diffraction pattern may show the continuous transform and always shows an averaged view. However, the individual reflections from a single crystal are a sampling of the continuous Fourier transform at discrete points in a single plane rather than an averaged view. It should be noted that other features are also present in the diffraction pattern that do not arise from a simple helical structure. This is especially true along the equator of Fig. 2. Since the helical portion of the structure has repeating structural elements, it gives rise to a relative enhancement of the diffraction pattern and so makes it possible to recognize the helical components of the pattern. The distribution of diffraction intensity along oblique lines, as in regions (*b*) and (*c*) in Fig. 2, is due to the fact that the ribose-phosphate backbones of the helical nucleic acids cross each other, while the near meridional reflections in region (*a*) are due to the hydrogen-bonded purine and pyrimidine bases that are stacked in the center of the helical structure. In the diffraction pattern of Fig. 2, the reflections in the 3- to 4-Å region are off-meridional due to the fact that the bases are tilted away from an orientation at right angles to the helix axis, as is found in the A form of DNA (9). In some respects, the pattern in Fig. 2 has similarities to that found in the double-helical RNA molecules (10–12). However, it is difficult to make a detailed comparison because of the additional diffraction data present in Fig. 2.

If a fiber of helical nucleic acid is rotated about the fiber axis, the diffraction pattern does not change. However, this is not true for crystalline transfer RNA. Fig. 3 shows a diffraction pattern taken along the *b*-axis, in which the *c*-axis is in the vertical direction as in Fig. 2. Here the diffraction pattern has more intense reflections in a central oval region but does not have a distribution that can be recognized as characteristic of a helical molecule. At first this suggests a paradox, in that the molecule appears to be both helical and nonhelical depending upon the direction from which one is viewing the structure. However, this effect can be readily understood. The diffraction pattern of a helical molecule appears the same when visualized from various angles around the helix axis because the molecule looks the same at these angles. However, the fact that the diffraction pattern differs in the case of crystalline transfer RNA suggests that the helical regions of the molecule do not appear the same while looking along the *b*-axis as they do while looking along the *a*-axis. This effect would be expected if the helical portion of the molecule had a length less than one complete turn. In particular, a large part of the helical diffraction pattern is due to the two chains crossing each other; a short helical segment does not appear to have chains that cross each other in all views. As viewed in one projection, a half-turn of a double helix has two strands crossing each other, thus a diffraction pattern viewed in this direction would have a distribution of diffraction intensity largely characteristic of the helix. On the other hand, a rotation of 90° about the helix axis would produce a view where the two chains are running approximately in the same direction. A short double-helical segment would, therefore, produce different diffraction patterns at different orientations about the helix axis.

We have confirmed these qualitative arguments by calculating the Fourier transform of short segments of double-helical RNA models. When the transform of one complete turn of a helix is calculated, the diffraction pattern is very similar when viewed from two directions that are 90° apart, and the distribution is characteristic of a helix. However, the transform of a half-helix containing six base pairs does not look the same in two different projections, 90° apart, around the helix axis. The calculated intensity shows a more helical distribution when the two ribose-phosphate chain segments cross each other in projection; the transform viewed 90° away does not have an overtly helical distribution. Thus, we can account simply for the observed features of the diffraction pattern by suggesting that they arise from short segments of double-helical RNA from within the transfer RNA molecule.

DISCUSSION

These observations represent in no sense a solution of the diffraction pattern of crystalline transfer RNA. Rather they point out that certain features of the diffraction pattern can be readily understood by recognizing the fact that they arise from short double-helical fragments, approximately a half-helical turn in length. In the tRNA molecule, these segments would be seen with their ribose-phosphate chains crossing each other when the molecule is viewed along the *a*-axis but not along the *b*-axis. At present, we can interpret the helical component of the diffraction pattern only in a qualitative sense.

Diffraction patterns of helical nucleic acids have been studied extensively for fibrous forms of DNA (8, 9), RNA (10–12), and various synthetic polynucleotides (8). Although these patterns have certain similar general features, there are considerable differences in detail, since the molecules themselves differ in diameter, helical pitch, and in the stacking and tilt of the paired purine·pyrimidine bases. From studies of double-stranded RNA from viral and other sources (10–13), it has been shown that the helical geometry of the molecule changes somewhat as the ionic environment is altered. Molecular models for double-helical RNA have been built containing 10 and 11 base pairs per turn (14). The calculated diffraction patterns for these two models show definite, but generally small, differences. Accordingly, we cannot interpret the data in Fig. 2 in terms of a detailed geometry for the helical segments of tRNA. Instead, we must await the solution of the entire crystal structure since it is virtually impossible to

clearly separate diffraction data arising from helical segments from that produced by the nonhelical regions.

Nonetheless, the observation that the helical pattern is not observable when one rotates the crystal (or molecule) 90° about the long axis of the unit cell provides some relevant information. It suggests that there are not long uninterrupted stretches of double helix in the molecule. However, short segments of approximately a half-helical turn would produce this effect. If there are several such segments in the molecule, it is likely that they are roughly aligned with each other so that the crossed polynucleotide chains are predominantly visible along one direction. This is a qualitative constraint and provides only limited information about the molecule. It does, however, provide some direct physical support for the cloverleaf formulation of the secondary structure of transfer RNA. This configuration suggests that there are four "stems", or double-helical regions, in the molecule that contain from 4–7 base pairs. These segments are approximately a half-helical turn in length.

Transfer RNA has been shown to crystallize in many different unit cells, and the crystals have varying degrees of resolution in their x-ray diffraction pattern. Our own experience with yeast phenylalanyl-tRNA bears this out, since we have found various crystal forms and unit cells for this molecule depending upon variations in crystallization conditions. At the same time, the resolution of the diffraction pattern also varies considerably. The great variety of crystal forms is probably due to the fact that the interactions between molecules in the lattice are few and rather nonspecific, so that variations in crystallizing conditions alter the packing. For the crystals reported here, we do not know which conditions are responsible for the high resolution of the diffraction pattern. It is possible that the cationic spermine plays an important role, although it has not had a similar effect in other attempts at tRNA crystallization. In any case, tRNA crystals that yield this high a resolution make it possible to look forward to obtaining electron-density maps of this molecule with the same degree of detail now available for many crystalline proteins.

We thank Harriett Greenwood for her enthusiastic assistance. This work was supported by research grants from the National Institutes of Health, the National Science Foundation, and the National Aeronautics and Space Administration.

1. Holley, R., J. Apgar, G. Everett, J. Madison, M. Marquisee, S. Merrill, J. Penswick, and A. Zamir, *Science*, **147**, 1462 (1965).
2. Kim, S. H., and A. Rich, *Science*, **162**, 1381 (1968).
3. Hampel, A., M. Labanauskas, P. G. Connors, L. Kirkegard, U. L. Rajbhandary, P. B. Sigler, and R. Bock, *Science*, **162**, 1384 (1968).
4. Cramer, R., F. v. d. Haar, W. Saenger, and E. Schlimme, *Angew. Chem. Int. Ed. Engl.*, **7**, 895 (1968).
5. Fresco, J. R., R. D. Blake, and R. Langridge, *Nature*, **220**, 1285 (1968).
6. Kim, S. H., and A. Rich, *Science*, **166**, 1621 (1969).
7. Cochran, W., F. H. C. Crick, and V. Vand, *Acta Cryst.*, **5**, 581 (1952).
8. Davies, D. R., *Annu. Rev. Biochem.*, **36**, 321 (1967).
9. Langridge, R., H. Wilson, C. Hooper, M. Wilkins, and L. Hamilton, *J. Mol. Biol.*, **2**, 19 (1960).
10. Langridge, R., and P. Gomatos, *Science*, **141**, 694 (1963).
11. Tomita, K., and A. Rich, *Nature*, **171**, 737 (1964).
12. Sato, T., Y. Kyogoku, S. Higucki, Y. Mitsui, Y. Iitaka, M. Tsuboi, and K. Miura, *J. Mol. Biol.*, **16**, 180 (1966).
13. Arnott, S., W. Fuller, A. Hodgson, and I. Prutton, *Nature*, **220**, 561 (1968).
14. Arnott, S., *Progr. Biophys. Mol. Biol.*, **21**, 265 (1970).